Electronic Supplementary Material (ESI) for Analytical Methods.

Supplementary information

Body composition analysis via spatially resolved NIR spectroscopy with multifrequency bioimpedance precision

Evgeny Shirshin[a,b,†], Boris Yakimov[a,c†], Denis Davydov[a,c], Alexey Baev[a], Gleb Budylin[c], Nikolay Fadeev[a], Liliya Urusova[b], Nano Pachuashvili[b], Olga Vasyukova[b], Natalia Mokrysheva[b]

a. Faculty of Physics, M.V. Lomonosov Moscow State University, 1-2 Leninskie Gory, 119991 Moscow, Russia

b. Endocrinology Research Centre, Dmitriya Ulianova Street, 11, 117036 Moscow, Russia

c. Laboratory of Clinical Biophotonics, Biomedical Science and Technology Park, Sechenov First Moscow State Medical University, Trubetskaya 8, Moscow, 119048, Russia

† Contributed equally

Cohort description

A total of 292 subjects (102 males and 190 females) participated in a simultaneous multifrequency bioelectrical impedance analysis (MF-BIA) and near-infrared diffuse reflectance spectroscopy study. The mean body mass index (BMI) of the participant was 24 ± 5.4 kg/m^2 spanning from 17 kg/m^2 to 49.7 kg/m^2. All participants completed the study voluntarily and were informed about the purposes of the study. All measurements were non-invasive and did not require confirmation by an ethics committee.

Bioelectrical Impedance Analysis

To assess tissue composition, InBody-770 MF-BIA device (Biospace Co.) was used. Measurements using the device were carried out according to the manufacturer's recommendations. Subjects stood with their bare feet on the device's scales, with their feet positioned on the corresponding electrodes. Hands with clamped electrodes were spread straight apart from torso at an angle of about 15-30 degrees. Weight was estimated using this device; height and gender were indicated in the device as part of the measurement and were then used to calculate the participant's BMI.

To calculate fat content and soft lean mass percentage, the corresponding absolute fat and lean mass values calculated by the device were divided by the participant's weight and multiplied by 100.

Diffuse reflectance spectroscopy measurement

The device used to measure spatially resolved diffuse reflectance spectra is described in detail in [1]. Briefly, measurement part of the device consisted of two optical fibers with a core diameter of 550 µm, detecting a diffuse reflection signal from the skin at different distances between the source and detector in the spectral range of 800–1100 nm. Source detector separation (SDS) was controlled by a linear translation stage (ELL17/M Stage, Thorlabs, United States) and varied from 0 to 15 mm in 1 mm steps. One of the fibers was connected to a broadband source (SLS201 lamps, Thorlabs USA) used to illuminate the tissue site, while the other fiber was connected to a Maya 2000 Pro spectrometer (Ocean Optics, USA) and acted as a detector.

The effective optical density (OD) spectrum was calculated as follows:

$$OD(\lambda) = -\ln\left(\frac{I(\lambda) - I_{bg}(\lambda)}{I_{ref}(\lambda) - I_{bg}(\lambda)}\right)$$

where $I(\lambda)$ is the signal intensity of the sample, $I_{bg}(\lambda)$ is the background signal, and $I_{ref}(\lambda)$is the signal intensity from the reference sample (LabSphere, United States). To standardize the spectra and estimate the absorption value, after obtaining the diffuse reflectance spectrum, the OD values averaged over the wavelength range 855-865 nm was subtracted from the OD spectrum to take into account differences in the differences in diffuse reflectance of the skin of different patients.

The skin of the inner side of the forearm at a distance of approximately 5-10 cm from the elbow without visible vessels was used as a measurement site. The optical fibers were located perpendicular to the skin surface in all experiments.

Model training and validation

To train and evaluate statistical models predicting fat and soft lean mass percentages estimated using MF-BIA, we used simple predictors extracted from OD spectra and physiological data of patients (gender, age, body mass index). As optical descriptors, we used the values OD_λ as the average optical density value in the range (λ - 5 nm, λ + 5 nm).

We considered three sets of descriptors:

- Simple NIRS descriptors: OD at wavelengths 930 and 970 nm at SDS = 10 mm,
- “advanced” NIRS descriptors: OD values at 890, 930, 970, 1015, 1050 nm and at SDS varying from 2 to 14 mm in increments of 2 mm;
- Combined optical and physiological features: BMI, sex, weight, age and optical densities at 930 and 970 nm at SDS of 4, 10 and 14 mm. BMI was additionally transformed to BMI^{-1}, while sex was one-hot encoded (“Female” = 1, “Male” = 0).

As a base model we used a linear regression with an additional combination of L_1 and L_2 regularizations (“elastic net” term) to eliminate the problem of multicollinearity in the features. For each of the models, we additionally tuned the total contribution of regularization to the loss and the L_1-ratio the regularization term in 7-fold random cross-validation on the input data. All the input features were preliminary normalized by substracting median value of the feature and divided by the interquartile range of the feature on the training set.

Although it is typical to tune hyperparameters of the model and assess final quality using different validation and test sets, we believe that a small number of tuned hyperparameters while using 7-fold cross-validation with random shuffling minimized the risk of overfitting during the hyperparameter optimization stage algorithm. Thus, we tuned hyperparameters using 7-fold cross-validation with randomly shuffled objects of the full dataset and then assessed final quality using differently shuffled 7-fold splits.

The models' performance was assessed using the mean absolute error (MAE) calculated on the validation subsets. Additionally, the Pearson correlation coefficients are presented, calculated between predicted and true values of the target variable.

Data processing and model building were carried out using custom scripts in Python 3 using the libraries Numpy, Pandas, Matplotlib, Scikit-learn [2]. The feature importances were assessed as Shapley values using the Shap package [3].

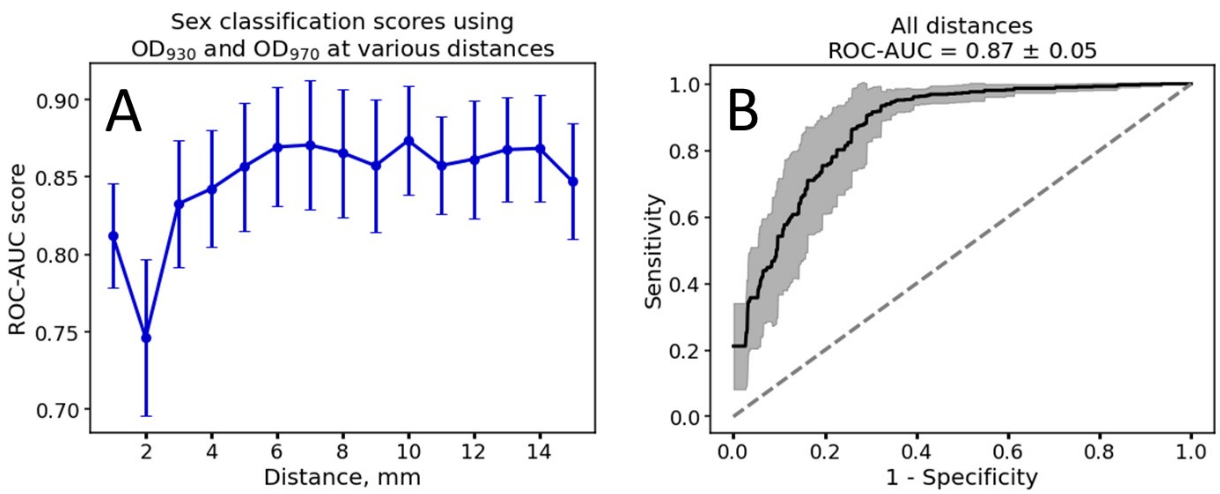

Figure S1 – A) Dependence of ROC-AUC score of volunteers' classification by sex using OD_{930} and OD_{970} data at different source-detector separation distances. B) ROC-curve for a volunteers' classifier by sex, trained using OD_{930} and OD_{970} values for source-detector separation distances varied from 1 to 15 mm in 1 mm step.

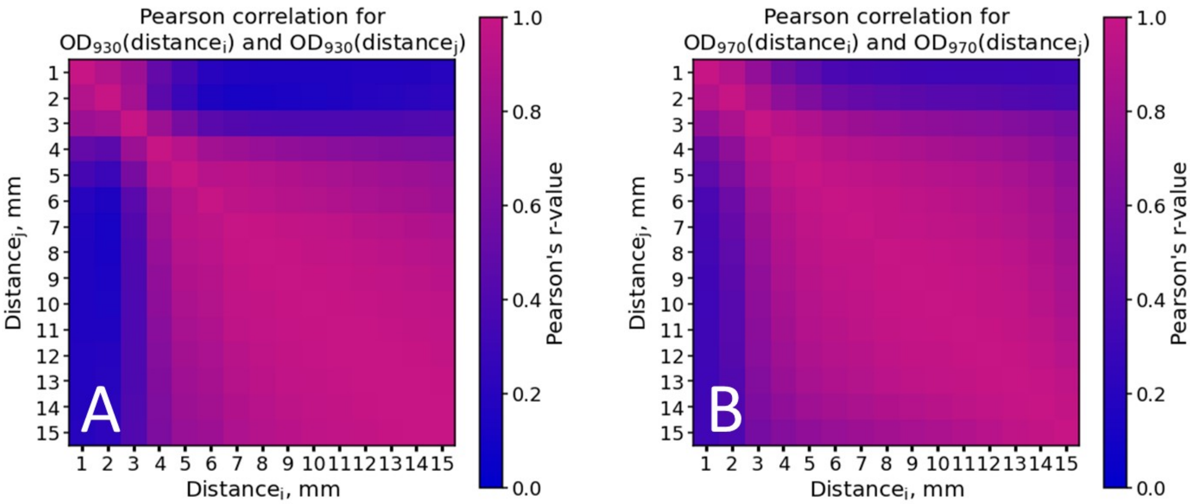

Figure S2 – Maps of Pearson r-values for optical density OD values at wavelengths 930 nm (A) and wavelengths 970 nm (B), obtained for various distances between the source and detector.

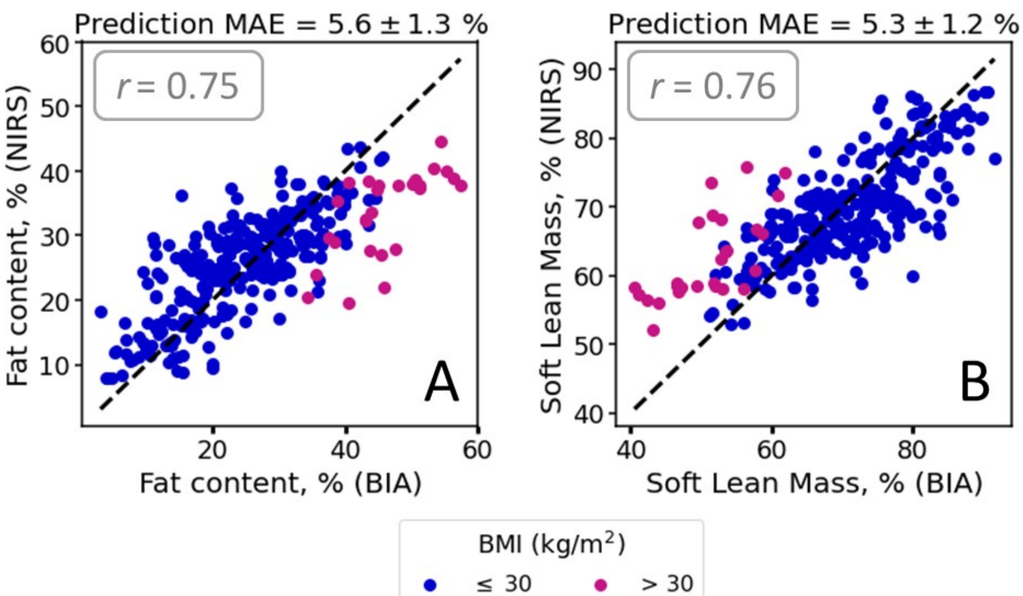

Figure S3 – Predictions of fat (A) and lean mass percentage (B) using NIRS “classical” features: OD values at 930 and 970 nm for single source detector separation equals 10 mm.

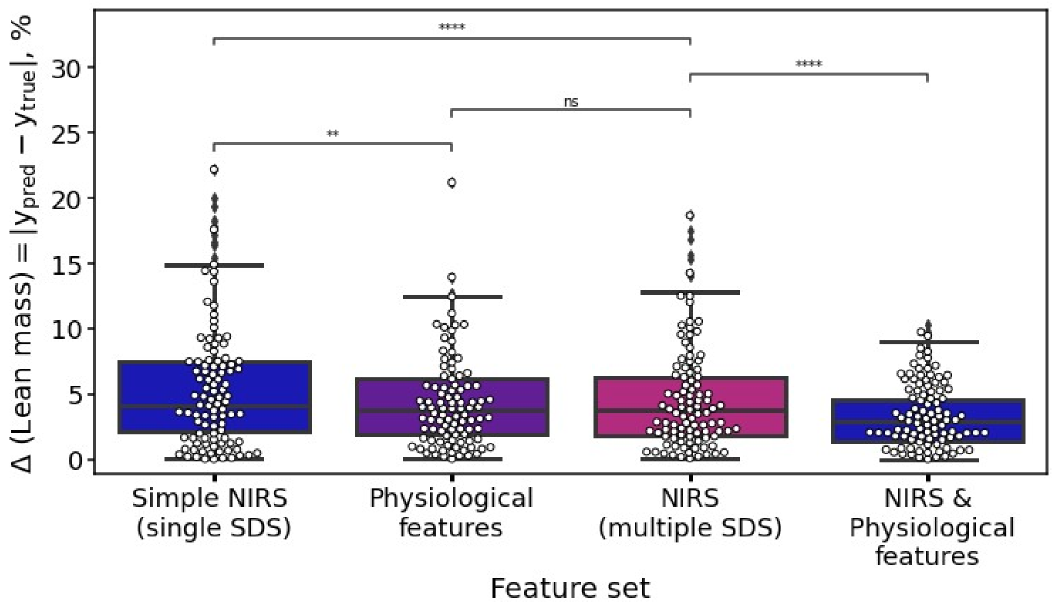

Figure S4 – Absolute values of prediction residuals obtained in 7-fold cross-validation for best models trained using different feature sets: simple and “advanced” NIRS features, purely physiological features (BMI, etc.) and combination of NIRS and physiological features. Residuals are compared using T-test for related samples with additional Bonferroni multiple comparisons correction. “**” indicate $p < 10^{-2}$, “****” indicate $p < 10^{-4}$.

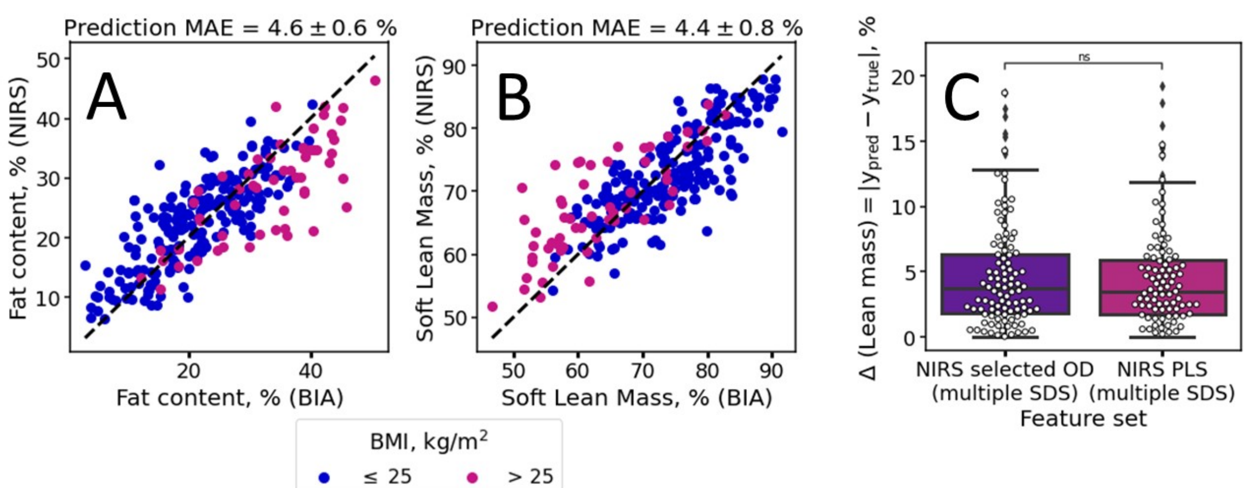

Figure S5 — A,B) The dependence of predicted fat content and lean mass using PLS-model, trained on NIRS spectra obtained for SDS in the range from with linear regression model and PLS-regression model.

References

[1] Davydov, D. A., Budylin, G. S., Baev, A. V., Vaypan, D. V., Seredenina, E. M., Matskeplishvili, S. T., ... & Shirshin, E. A. (2023). Monitoring the skin structure during edema in vivo with spatially resolved diffuse reflectance spectroscopy. *Journal of Biomedical Optics*, *28*(5), 057002-057002.

[2] Pedregosa, F., Varoquaux, G., Gramfort, A., Michel, V., Thirion, B., Grisel, O., ... & Duchesnay, É. (2011). Scikit-learn: Machine learning in Python. the Journal of machine Learning research, 12, 2825-2830.

[3] Lundberg, S. M., Nair, B., Vavilala, M. S., Horibe, M., Eisses, M. J., Adams, T., ... & Lee, S. I. (2018). Explainable machine-learning predictions for the prevention of hypoxaemia during surgery. Nature biomedical engineering, 2(10), 749-760.